AIAA JOURNAL
Vol. 39, No. 4, April 2001

Effect of Residual Stresses on Buckling Localization in a Cylindrical Panel

V. Tvergaard*
Technical University of Denmark, 2800 Lyngby, Denmark
and
A. Needleman†
Brown University, Providence, Rhode Island 02912

Localization, in the sense of a more or less abrupt change from a smoothly varying deformation pattern to a pattern involving one or more regions of highly localized deformation, occurs in a wide variety of circumstances, including shear band localizations in structural metals, rocks, and concrete and localized tearing in sheet forming operations. The onset of necking in the round bar tensile test is a classic example of this type of localization. A similar observation in structural buckling is that the final buckled configuration is a localized mode in contrast to the periodic mode associated with the critical buckling load. In buckling, as in tensile necking, the basic mechanism of localization is associated with a bifurcation in the vicinity of the maximum load point. In particular, narrow cylindrical panels occur in stiffened cylindrical shells and, depending on their curvature, may or may not have a load maximum associated with deformation in the periodic buckling mode. Previously we analyzed the development of buckling pattern localization in elastic–plastic cylindrical panels subject to axial compression. The effect of residual stresses on buckling localization in cylindrical panels is now explored.

Nomenclature

a	=	length of shell analyzed
$a_{\alpha\beta}$	=	metric tensor of the shell middle surface
b	=	distance between shell stiffeners
$d_{\alpha\beta}$	=	curvature tensor of the shell middle surface
E	=	Young's modulus
h	=	shell thickness
K	=	tangent stiffness
L, L_A, L_B	=	bar lengths
L^{ijkl}	=	tensor of instantaneous moduli
$M^{\alpha\beta}$	=	moment tensor
m	=	buckling mode wavelength
N	=	bar axial force
$N^{\alpha\beta}$	=	membrane stress tensor
n	=	strain hardening exponent
P	=	shell axial load
R	=	shell radius
U	=	magnitude of shell axial end displacement
u	=	bar displacement
u_α	=	shell in-plane displacements
w	=	shell out-of-plane displacement
x	=	bar axial coordinate
x^α	=	coordinates in shell middle surface
x^3	=	shell through-thickness coordinate
α	=	axial buckling mode wavelength parameter, mb/a
β	=	parameter characterizing the residual stress distribution
ϵ	=	strain
$\epsilon_{\rm av}$	=	shell average axial strain
$\epsilon_{\alpha\beta}$	=	membrane strain tensor
η_{ij}	=	Lagrangian strain tensor
θ	=	geometrical parameter
$\kappa_{\alpha\beta}$	=	bending strain tensor
ν	=	Poisson's ratio
$\bar{\xi}$, $\bar{\xi}_1$	=	imperfection amplitudes
ρ	=	the ratio L_B/L
$\sigma_{\rm av}$	=	shell average axial stress
σ_c	=	critical buckling stress
σ^{ij}	=	stress tensor
σ_R	=	residual stress amplitude
σ_y	=	yield strength

Subscript and Superscript

$,\alpha$	=	surface covariant derivative
$\dot{}$	=	time derivative

I. Introduction

A COMMON occurrence in a wide variety of circumstances is that a smoothly varying deformation pattern changes more or less abruptly to one involving regions of highly localized deformation. Examples include shear band localizations in structural metals, rocks, and concrete and localized tearing in sheet forming operations. Considére's result[1] that necking initiates at the maximum load point for a sufficiently long thin bar is a classic illustration of this type of localization.

In structural buckling, the final buckled configuration is often seen to be a localized mode in contrast to the periodic mode associated with the critical buckling load. The experiments of Moxham[2] show that the final collapse mode of an axially compressed steel plate strip involves one buckle rather than a periodic pattern. Tvergaard and Needleman[3] observed that the basic mechanism of buckling localization is associated with a bifurcation in the vicinity of the maximum load point and is closely analogous to the Considére[1] view of tensile necking.

A variety of buckling phenomena can be understood in terms of a bifurcation into a localized mode at, or subsequent to, the attainment of a load maximum. Cylindrical shells and panels are basic structural elements of considerable technological importance that have been the subject of many fundamental investigations, for example, that of Amazigo and Budiansky,[4] and that can exhibit localization. For example, relatively thick axially compressed circular cylindrical shells collapse axisymmetrically, whereas thinner shells buckle in a diamond pattern. In all cases, the initial buckling mode for elastic–plastic circular cylindrical shells is axisymmetric. In the plastic range, the critical stress for nonaxisymmetric modes is slightly higher than the critical stress for the axisymmetric mode. For thicker shells, bifurcation into a nonaxisymmetric mode occurs

Presented as Paper 2000-1462 at the AIAA 41st Structures, Structural Dynamics, and Materials Conference, Atlanta, GA, 3–6 April 2000; received 1 June 2000; revision received 26 September 2000; accepted for publication 26 September 2000.

*Professor, Department of Solid Mechanics.
†Professor, Division of Engineering.

after a load maximum has been attained.[5,6] Localization following the load maximum for thicker shells is what precludes the nonaxisymmetric bifurcation and causes collapse to occur in an axisymmetric mode.[7,8]

Narrow cylindrical panels occur in stiffened cylindrical shells. Koiter[9] showed, on the basis of his general theory of elastic stability,[10] that whether or not a load maximum is attained for such panels depends on the panel curvature. Sufficiently flat elastic cylindrical panels subject to axial compression have a stable initial postbuckling response and so do not attain a load maximum in the vicinity of the bifurcation point. On the other hand, more curved panels have an initially unstable postbuckling response, and a load maximum is attained in the vicinity of the bifurcation point. Hence, such panels are imperfection sensitive. Tvergaard[11] analyzed the postbuckling behavior and imperfection sensitivity of elastic–plastic cylindrical panels. The decrease in stiffness associated with plastic yielding increased the range of panel curvatures that gives rise to imperfection sensitive response. Thus, whether or not a cylindrical panel is prone to localization depends on the panel curvature and, for elastic–plastic panels, on the strain hardening characteristics of the material.

Recently, Tvergaard and Needleman[12] analyzed the development of buckling pattern localization in elastic–plastic cylindrical panels subject to axial compression. For the cylindrical panel, it was shown that buckling localization develops shortly after a maximum load has been attained, and this occurs for a purely elastic panel as well as for elastic–plastic panels. When localization occurs after a load maximum, but where subsequently the load starts to increase again, it was found that near the local load minimum the buckling pattern switches back to a periodic type of pattern. The inelastic material behavior of the panel was described in terms of the J_2-corner theory of Christoffersen and Hutchinson,[13] which is a phenomenological theory of plasticity of a class considered by Sanders[14] that avoids the sometimes unrealistically high buckling loads predicted by smooth yield surface theories of plasticity.

In this paper, we first present a simple model for buckling localization. Then, the effect of residual stresses on buckling mode localization in cylindrical panels is analyzed. Ravn-Jensen and Tvergaard[15] showed that residual stresses can significantly affect the maximum load in cylindrical shell structures and so can be expected to have an effect on buckling localization. Here, this effect is illustrated for the case of cylindrical panels.

II. Simple Model

A simple one-dimensional bar model[3] illustrates that the basic mechanism involved in buckling localization is analogous to the necking of tensile bars. A homogeneous, axially compressed bar constrained to remain straight, as shown in Fig. 1, is used as a one-dimensional model of a periodically buckled structure. The bar is of length L, and end displacements are prescribed at $x = 0, L$. The incremental relation between the axial force N and the strain ϵ is

$$\dot{N} = K\dot{\epsilon}, \qquad \dot{\epsilon} = \dot{u}_{,x} \tag{1}$$

where subscript $,x$ denotes differentiation with respect to the axial coordinate x, the overdot denotes incremental quantities, and K is the tangent stiffness, which incorporates the effects of both geometric and material nonlinearities.

Incremental equilibrium requires

$$\dot{N}_{,x} = 0 \tag{2}$$

At any stage of loading, one possible solution is continued homogeneous deformation. The possibility of a bifurcation from the homogeneous state is sought where the bifurcation mode consists of a localized region that can undergo incremental straining different from that in the bulk, although each region itself deforms homogeneously.

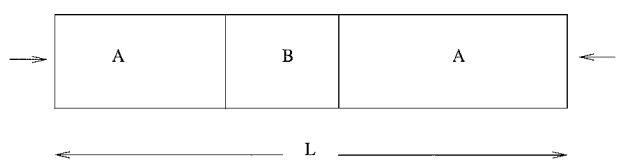

Fig. 1 One-dimensional bar model.

From Eq. (2),

$$\dot{N}_A = \dot{N}_B = \dot{N} \tag{3}$$

where the subscripts A and B are quantities outside and inside the localized region, respectively.

Since

$$\dot{N}_A = K\dot{\epsilon}_A, \qquad \dot{N}_B = K\dot{\epsilon}_B \tag{4}$$

incremental equilibrium implies

$$K(\dot{\epsilon}_A - \dot{\epsilon}_B) = 0 \tag{5}$$

Hence, the onset of localization is only possible at the maximum load point, that is, when $K = 0$.

The postlocalization response can be determined within the context of this bar model. Let L_A and L_B be the lengths associated with regions A and B, respectively. Then,

$$L = L_A + L_B \tag{6}$$

Because $\epsilon = \Delta u/\Delta x$,

$$\dot{\epsilon} = (1 - \rho)\dot{\epsilon}_A + \rho\dot{\epsilon}_B \tag{7}$$

where $\rho = L_B/L$.

After localization, the constitutive response is expressed by

$$\dot{N}_A = K_A\dot{\epsilon}_A, \qquad \dot{N}_B = K_B\dot{\epsilon}_B \tag{8}$$

Combining Eqs. (8), (7), and (3) gives

$$\dot{\epsilon} = (\dot{N}/K_B)\ \rho + (1 - \rho)(K_B/K_A)] \tag{9}$$

At localization $K_B = 0$, whereas K_B is negative after the maximum load. With K_A algebraically larger than K_B, the postlocalization traction-deformation gradient curve lies below the one for homogeneous straining and the smaller ρ is the more quickly the load drops. Hence, the postlocalization stiffness depends on the size scale of the localized region, and this length scale is set by factors outside the scope of the one-dimensional analysis. For localized buckling in structures, geometric effects set the size scale. This simple model illustrates the tendency for localization when a load maximum is reached and has bearing on a variety of buckling problems including, for example, the axially compressed plate strips of Ref. 2, stiffened panels, bent tubes that reach a maximum load due to the Brazier effect (ovalization of the cross section), and the axially compressed cylindrical panels analyzed here.

III. Governing Equations

The axially compressed cylindrical panels to be analyzed here are taken to be part of a longitudinally stiffened cylindrical shell, each of which is bounded by two neighboring stiffeners. The local buckling mode of interest is one in which the stiffeners remain straight, while the shell buckles in a short wave pattern between the stiffeners. The initial elastic postbuckling behavior of such panels was analyzed by Koiter,[10] and it was shown that the postbuckling behavior is stable for sufficiently flat panels, as for elastic plates, but unstable for more curved panels. A similar transition from platelike behavior for rather flat panels to more unstable behavior for curved panels was shown by Tvergaard[11] for elastic–plastic cylindrical panels. Here, with a focus on buckling localization, the main interest is in cases where the primary periodic buckling pattern is characterized by an unstable postbuckling behavior.

The formulation of the governing equations follows that by Tvergaard and Needleman[12] and is outlined here. The shell has thickness h and radius R, and the circumferential distance between the equally spaced stiffeners is b (Fig. 2). The main effect of the stiffeners is to prevent waviness of radial deflections along their lines of attachment. As in Koiter's analysis of the elastic cylindrical panel,[10] this is the only stiffener constraint accounted for in the

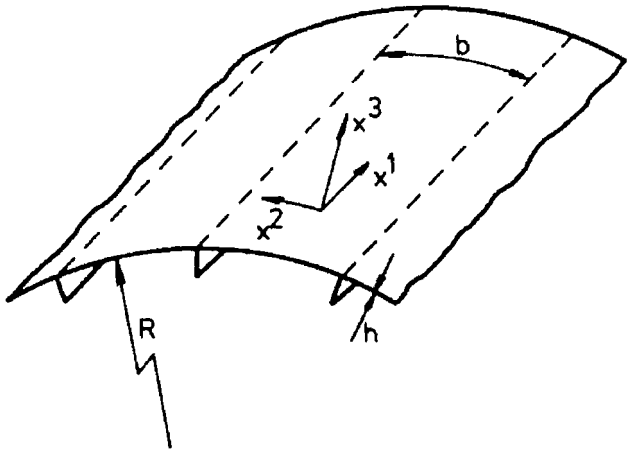

Fig. 2 Cylindrical panel.

present investigation. Thus, it is assumed that there is no constraint on tangential shell displacements along the stiffeners. The torsional rigidity of the stiffeners is also neglected. On the middle surface of the circular cylindrical shell, a point is identified by the coordinates x^1 and x^2, where x^1 measures the distance along the cylinder axis and x^2 measures distance in the circumferential direction. The displacement components are u^α on the surface base vectors and w on the outward surface normal. The strain measures used are the nonlinear membrane strain tensor

$$\epsilon_{\alpha\beta} = \tfrac{1}{2}(u_{\alpha,\beta} + u_{\beta,\alpha}) - d_{\alpha\beta}w + \tfrac{1}{2}a^{\gamma\delta}(u_{\gamma,\alpha} - d_{\gamma\alpha}w)(u_{\delta,\beta} - d_{\delta\beta}w) + \tfrac{1}{2}\big(w_{,\alpha} + d^\gamma_\alpha u_\gamma\big)\big(w_{,\beta} + d^\delta_\beta u_\delta\big) \tag{10}$$

and the linear bending strain tensor specified by Koiter[16]

$$\kappa_{\alpha\beta} = \tfrac{1}{2}\Big[\big(w_{,\alpha} + d^\gamma_\alpha u_\gamma\big)_{,\beta} + \big(w_{,\beta} + d^\delta_\beta u_\delta\big)_{,\alpha} - \tfrac{1}{2}d^\gamma_\alpha(u_{\beta,\gamma} - u_{\gamma,\beta}) - \tfrac{1}{2}d^\gamma_\beta(u_{\alpha,\gamma} - u_{\gamma,\alpha})\Big] \tag{11}$$

where $a_{\alpha\beta}$ and $d_{\alpha\beta}$ are the metric tensor and the curvature tensor, respectively, of the undeformed middle surface, and subscript $,\alpha$ denotes covariant differentiation. Greek indices range from 1 to 2, whereas Latin indices (to be employed subsequently) range from 1 to 3, and the summation convention is adopted for repeated indices. Note that strain measures proposed by Niordson[17] are identical with Eqs. (10) and (11), except for small differences in the bending strain measure of the order of $d^\gamma_\alpha \epsilon_{\gamma\beta}$.

The three-dimensional constitutive relations are taken to be of the form

$$\dot\sigma^{ij} = L^{ijkl}\dot\eta_{kl} \tag{12}$$

where σ^{ij} is the stress tensor, η_{kl} is the strain tensor, and the overdot denotes an incremental quantity. Because the stress state in the shell is approximately plane, only the in-plane stresses enter into Eq. (12). Thus, the constitutive relations can be written as

$$\dot\sigma^{\alpha\beta} = \hat L^{\alpha\beta\gamma\delta}\dot\eta_{\gamma\delta}, \qquad \hat L^{\alpha\beta\gamma\delta} = L^{\alpha\beta\gamma\delta} - \frac{L^{\alpha\beta 33}L^{33\gamma\delta}}{L^{3333}} \tag{13}$$

The in-plane components of the Lagrangian strain tensor at a distance x^3 outward from the shell middle surface are approximated by

$$\eta_{\alpha\beta} = \epsilon_{\alpha\beta} - x^3\kappa_{\alpha\beta} \tag{14}$$

The membrane stress tensor $N^{\alpha\beta}$ and the moment tensor $M^{\alpha\beta}$ in a shell with thickness h are taken to be

$$N^{\alpha\beta} = \int_{-h/2}^{h/2}\sigma^{\alpha\beta}\,\mathrm{d}x^3, \qquad M^{\alpha\beta} = -\int_{-h/2}^{h/2}\sigma^{\alpha\beta}x^3\,\mathrm{d}x^3 \tag{15}$$

Then, from Eqs. (13–15), incremental relations are obtained for $\dot N^{\alpha\beta}$ and $\dot M^{\alpha\beta}$ in terms of $\dot\epsilon_{\gamma\delta}$ and $\dot\kappa_{\gamma\delta}$. The requirement of equilibrium is specified in terms of the principle of virtual work

$$\int_A \big[N^{\alpha\beta}\delta\epsilon_{\alpha\beta} + M^{\alpha\beta}\delta\kappa_{\alpha\beta}\big]\,\mathrm{d}A = P\delta U \tag{16}$$

where A is the middle surface area, P is the total axial load acting on the cylinder, and U is the axial displacement at one end ($x^1 = a$), while at the other cylinder end zero axial displacement is prescribed.

Because the buckling pattern is periodic in the circumferential direction, due to the constant stiffener spacing, only a shell section between the centers $x^2 = 0, b$ of the two neighboring cylindrical panels needs to be considered (see the coordinate system in Fig. 2). Because of the symmetry of mode displacements about these panel centers, the boundary conditions can be specified as

$$\frac{\partial u_1}{\partial x^2} = u_2 = \frac{\partial w}{\partial x^2} = \frac{\partial^3 w}{\partial (x^2)^3} = 0 \tag{17}$$

at $x^2 = 0, b$.

Across the line of attachment of a stiffener, continuity of all field quantities is required, except for the possible discontinuity of the transverse shear force resulting from the constraint

$$\frac{\partial w}{\partial x^1} = 0 \tag{18}$$

at $x^2 = b/2$.

The length of the shell section analyzed is a. The symmetry boundary conditions at $x^1 = 0$ are

$$u_1 = 0, \qquad \frac{\partial u_2}{\partial x^1} = \frac{\partial w}{\partial x^1} = \frac{\partial^3 w}{\partial (x^1)^3} = 0 \tag{19}$$

and at $x^1 = a$,

$$u_1 = -U, \qquad \frac{\partial u_2}{\partial x^1} = \frac{\partial w}{\partial x^1} = \frac{\partial^3 w}{\partial (x^1)^3} = 0 \tag{20}$$

so that $-U/a = \epsilon_{\mathrm{av}}$ is the specified average strain in the axial direction.

The uniaxial stress–strain curve is represented by a piecewise power law with continuous tangent modulus:

$$\epsilon = \begin{cases} \sigma/E, & \text{for } \sigma \le \sigma_y \\ (\sigma_y/E)\big[(\sigma/\sigma_y)^n(1/n) + 1\big], & \text{for } \sigma > \sigma_y \end{cases} \tag{21}$$

where n is the strain hardening exponent.

Bifurcation calculations based on the simplest deformation theory of plasticity are known to give better agreement with experimentally obtained buckling loads than do similar calculations based on the simplest flow theory because deformation theory accounts in a phenomenological way for the development of a yield surface vertex.[18] To account for the development of a vertex on subsequent yield surfaces, the analyses here are based on the J_2-corner theory of Christoffersen and Hutchinson.[19] In this theory, the instantaneous moduli for nearly proportional loading are chosen equal to the deformation theory moduli, and for increasing deviation from proportional loading the moduli increase smoothly until they coincide with the elastic moduli for stress increments directed along, or within, the corner of the yield surface. Details of the corner theory formulations in connection with buckling analyses have been given previously[6,20] and are not repeated here.

For an elastic cylindrical panel, Koiter[10] found the following expression for the critical bifurcation stress:

$$\sigma_c = -E\frac{\pi^2 h^2}{3(1-\nu^2)b^2}(1+\theta^4) \tag{22}$$

where the panel curvature parameter θ is defined by

$$\theta = \frac{\sqrt[4]{12(1-\nu^2)}}{2\pi}\frac{b}{\sqrt{Rh}} \tag{23}$$

Expression (22) is valid for $\theta \le 1$ with the axial half-wavelength equal to the panel width b. For $\theta > 1$ two axial wavelengths are critical simultaneously. For some of the cylindrical panels to be considered here, the elastic bifurcation stress (22) exceeds the initial yield stress. For these cases, the elastic–plastic bifurcation stress and the corresponding axial wavelength are determined by the use of expressions specified by Tvergaard.[11]

Numerical solutions of the incremental equilibrium equations are obtained by dividing the shell segment analyzed into rectangular conforming finite elements. Within an element, each displacement component is approximated by products of Hermitian cubics in the x^1 and x^2 directions, and integrals over the middle surface are evaluated by 4×4 point Gaussian quadrature, with seven-point Simpson integration through the thickness.

As long as the average axial shortening increases monotonically, the end displacement can be prescribed. However, after a load maximum, it is possible for the average axial strain rate to change sign. In such cases a special additional Rayleigh–Ritz procedure is used to prescribe a normal displacement increment instead of the end displacement.[21]

IV. Cylindrical Panel Results

Cylindrical panels with an initial imperfection are analyzed, where the imperfection is specified as an initial normal deflection of the form

$$\bar{w}(x^1, x^2) = \left[\bar{\xi} + \bar{\xi}_1 \cos(\pi x^1/a)\right] h \cos(m\pi x^1/a) \cos(\pi x^2/b) \tag{24}$$

where $\bar{\xi}$ is the amplitude of an initial periodic imperfection and the additional amplitude $\bar{\xi}_1$ specifies a small deviation from periodicity that makes the imperfection slightly larger near $x^1 = 0$ than near $x^1 = a$. The length of the shell section analyzed is taken to be $a = mb/\alpha$, where the axial wavelength parameter α is calculated so that the imperfection wavelength in the axial direction agrees with the wavelength of the critical bifurcation mode in an infinitely long panel, according to J_2-deformation theory of plasticity.

The residual stress distributions considered here are similar to those studied by Ravn-Jensen and Tvergaard,[15] that is, stress distributions corresponding to those resulting from welding along the stiffener (e.g., see Masubuchi[22]). When the structure is cooled to room temperature after welding, large tensile stresses develop along the weld as a result of thermal contraction, while compressive stresses develop farther away from the weld to keep equilibrium. It is assumed that the large initial tensile stress at the weld is equal to the initial yield stress σ_y, while the constant value of the stress component σ_{11} in a certain region between stiffeners is $-\sigma_R$. The transition of the axial stress component σ_{11} from the constant compressive level to the peak tensile residual stress is assumed to follow a cosine variation in a strip of shell material $\beta b/2$ wide on each side of the stiffener. Here, the value of the parameter β is simply determined by the residual stress field being self-equilibrated, that is, $\beta = 2\sigma_R/(\sigma_R + \sigma_y)$. Thus, when the residual stress level is specified by a small value of the stress ratio σ_R/σ_y, the transition takes place in a very narrow strip of shell material, whereas a larger residual stress ratio results in a transition over a wider strip of material.

The cylindrical panel to be used for illustration of the effect of residual stresses is one of those analyzed previously by Tvergaard and Needleman.[12] In this case, the material parameters are $\sigma_y/E = 0.002$, $\nu = 0.3$, and $n = 10$. The shell thickness to panel width ratio is taken to be $h/b = 0.025$, and b/R is specified by taking $\theta = 0.6$ in Eq. (23). Then, according to Tvergaard,[6] this is a case where an unstable postbuckling behavior is expected to lead to buckling localization. When $m = 6$ is taken in Eq. (24), a bifurcation analysis using expressions by Tvergaard[6] gives $\sigma_c/\sigma_y = -1.11$ and $\beta = 1.125$ for J_2-deformation theory. Note that $m = 6$ is a rather arbitrary choice of the panel length, but localization of a buckling pattern is more likely to occur in a structure containing several half-waves of the primary periodic buckling pattern. The initial imperfections are taken to be given by $\bar{\xi} = 0.01$ and $\bar{\xi}_1/\bar{\xi} = 0.01$ because it was found by Tvergaard and Needleman[12] in the absence of residual stresses that these small imperfections result in a clear case of buckling localization. The panel is analyzed here with a uniform mesh of 48×8 rectangular shell elements on the part of the cylindrical shell analyzed, that is, 48 elements in the longitudinal direction and 4 elements on either side of the stiffener between the stiffener and the centerline for the cylindrical panel (see Fig. 2). This 48×8 mesh is finer than the 24×4 mesh used in previous studies, which gives an improved resolution of the transition region for the residual stress distribution. The refined mesh makes only a little difference in the predictions, that is, an 0.5% reduction in the predicted maximum load and up to a 1.3% reduction in the load at a given average strain well beyond the maximum, but this slightly improves the possibility of detecting the onset of buckling pattern localization in a postbuckling range where there is only a slight downward slope of the overall stress–strain curve.

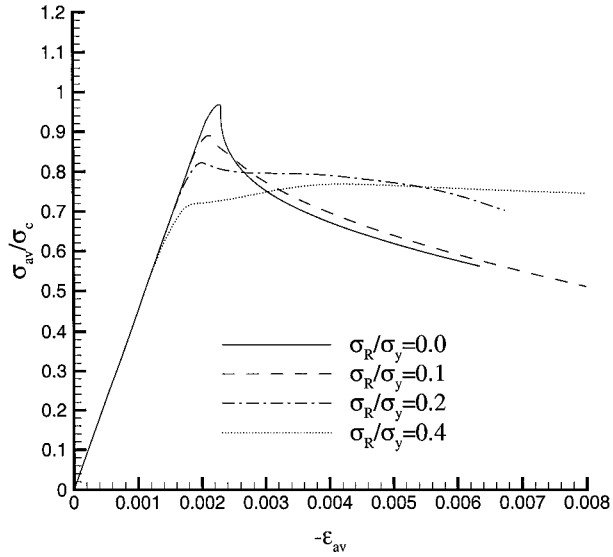

Fig. 3 Average axial stress curves for $\theta = 0.6$, $\bar{\xi} = 0.01$, and $\bar{\xi}_1/\bar{\xi} = 0.01$.

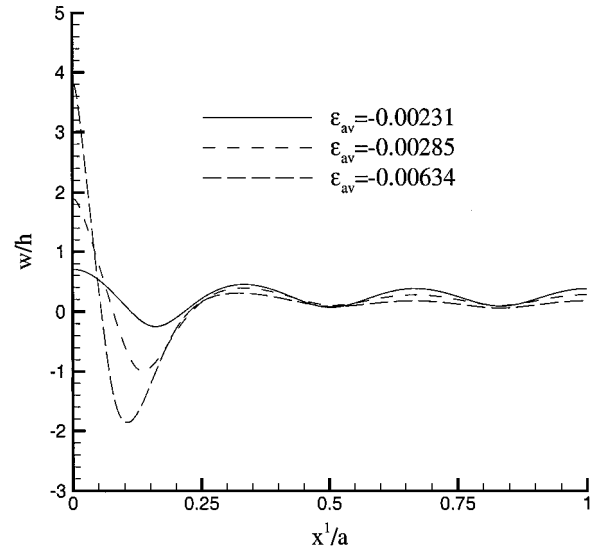

Fig. 4 Normal deflections along centerline, $x^2 = 0$, of a cylindrical panel with $\sigma_R/\sigma_y = 0.0$.

Figure 3 shows average axial stress–strain curves for different levels of the residual stress, where $\sigma_{av} = |P|/hb$ and $\epsilon_{av} = -U/a$. The solid curve, for $\sigma_R/\sigma_y = 0.0$, represents the case analyzed by Tvergaard and Needleman,[12] but here the computation is taken much farther. The other three curves correspond to increasing levels of initial residual stress, and they show the tendency, also found by Ravn-Jensen and Tvergaard,[15] that for a rather large residual stress level the initial load peak disappears, and buckling initially occurs under increasing load until a rather flat maximum is reached after some additional axial straining. Basically, the effect of the residual stresses is that the higher compressive stresses in the central part of a cylindrical panel will tend to reduce the buckling load and will also result in earlier onset of plastic yielding. The different behavior observed after the lower buckling load is a result of the interaction of the plastic yielding resulting from the residual stress field and that resulting from the postbuckling behavior.

Figures 4–7 show normal deflections along the centerline of the panel, $x^2 = 0$, to illustrate the buckling behavior. Figure 4 repeats

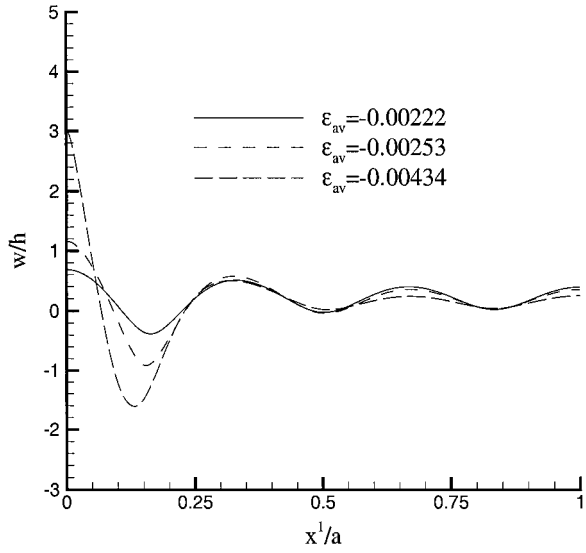

Fig. 5 Normal deflections along centerline, $x^2 = 0$, of a cylindrical panel with $\sigma_R/\sigma_y = 0.1$.

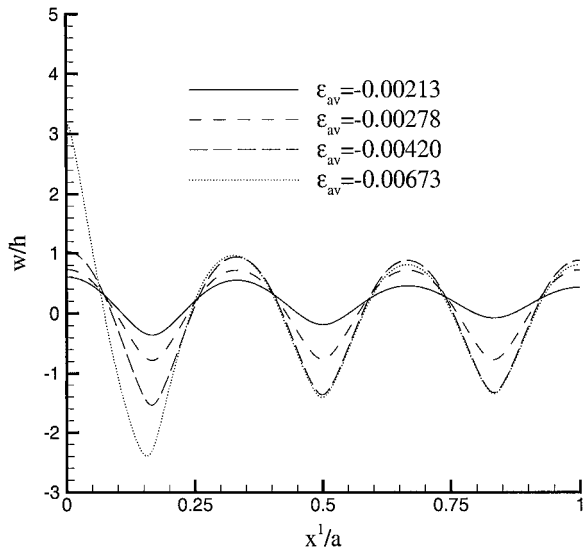

Fig. 6 Normal deflections along centerline, $x^2 = 0$, of a cylindrical panel with $\sigma_R/\sigma_y = 0.2$.

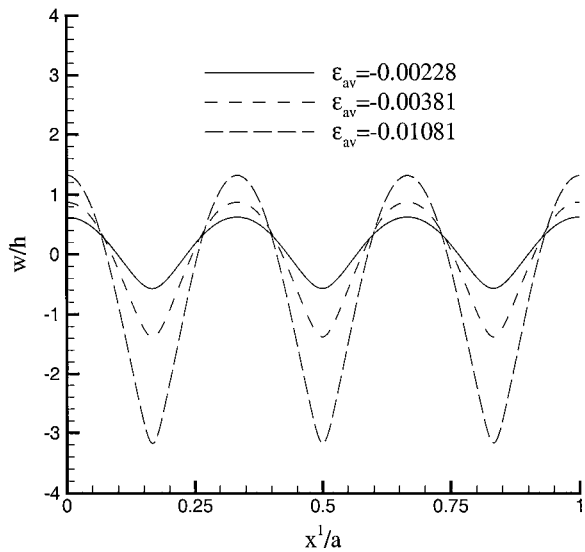

Fig. 7 Normal deflections along centerline, $x^2 = 0$, of a cylindrical panel with $\sigma_R/\sigma_y = 0.4$.

the result for the absence of residual stress, to show how the initially periodic buckling pattern develops into a clearly localized deflection pattern once the sharp load peak has been passed. For $\sigma_R/\sigma_y = 0.1$, the stress–strain curve in Fig. 3 also shows a rather sharp load peak, and the corresponding localization pattern in Fig. 5 is rather similar to that shown in Fig. 4. In the case of $\sigma_R/\sigma_y = 0.2$, the shape of the average stress–strain curve has started to change significantly, and this has a strong effect on the deflection pattern shown in Fig. 6. At $\epsilon_{av} = -0.00213$, just after the load maximum, some localization has started to develop, but at $\epsilon_{av} = -0.00278$, where the average stress strain curve has flattened out, this buckling pattern localization has disappeared. Subsequently, the downward slope of the average stress–strain curve increases again, as the effect of the initial residual stresses is wiped out by general plastic flow in the cylindrical panel, and then localization develops again, as is seen for the two larger values of ϵ_{av} in Fig. 6. Finally, for the largest residual stress value considered, Fig. 7 shows that no localization develops at all, even though a load maximum is passed in the post-buckling range at $\epsilon_{av} = -0.00419$. According to the simple model Eqs. (1–9)], localization should take place at the load maximum, but here the finite length of the panel analyzed, as compared with the buckle wavelength, gives a delay in the development of localization, and the downward slope of the stress–strain curve after the maximum is not large enough to overcome this delay.

The effect of residual stresses on buckling localization presented in Figs. 3–7 is not general for a wide range of cylindrical panels. Buckling localization can only occur if a load maximum has been reached, and this will only occur for certain combinations of panel geometry and material parameters.[11] However, even in such cases the localization behavior varies from case to case, as has been discussed by Tvergaard and Needleman.[12] To get some further understanding of the effect of residual stresses, another panel has been analyzed, with the same imperfections and axial wave number, but for a higher hardening material, $n = 3$, and with the curvature parameter $\theta = 0.75$, leading to $\sigma_c/\sigma_y = -1.32$. This case also gives some buckling localization[12] for $\sigma_R/\sigma_y = 0.0$. Even for the rather large residual stress, $\sigma_R/\sigma_y = 0.4$, where no localization occurred for the case studied earlier, it is found that this high hardening case gives localization as the load decays sharply immediately after the load maximum, but shortly after this, all localization is wiped out as the load starts to increase further, due to the high hardening. This illustrates how the localization behavior varies significantly with the problem parameters.

V. Conclusions

As described by the simple one-dimensional model, localization is predicted if a load maximum occurs, which includes load maxima predicted for purely elastic structures. However, material nonlinearity tends to soften the structural response, so that a structure with no maximum in the elastic range may show a maximum in the plastic range, and therefore, the nonlinear material behavior may strongly promote the localization process. With the residual stress distributions here, the load decreases more slowly after the peak load, as the magnitude of the residual stress increases. For a large enough residual stress, the postpeak decrease in load is sufficiently gradual that localization is suppressed for the low hardening finite length panels analyzed. However, changes in both material and geometric parameters strongly affect the postlocalization behavior and, hence, the influence of residual stresses.

References

[1] Considére, M., "L'Emploi du Fer et de l'Acier dans les Constructions," *Annales des Ponts et Chaussées*, Vol. 9, 1885, pp. 574–775.

[2] Moxham, K. E., "Buckling Tests on Individual Welded Steel Plates in Compression," Engineering Dept., Rept. CUED/C-Struct/TR 3 Cambridge Univ., Cambridge, England, U.K., 1971.

[3] Tvergaard, V., and Needleman, A., "On the Localization of Buckling Patterns," *Journal of Applied Mechanics*, Vol. 47, Sept. 1980, pp. 613–619.

[4] Amazigo, J. C., and Budiansky, B., "Asymptotic Formulas for the Buckling Stresses of Axially Compressed Cylinders with Localized or Random Imperfections," *Journal of Applied Mechanics*, Vol. 39, March 1972, pp. 179–184.

[5] Gellin, S., "Effect of an Axisymmetric Imperfection on the Plastic Buckling of an Axially Compressed Cylindrical Shell," *Journal of Applied Mechanics*, Vol. 46, March 1979, pp. 125–131.

[6]Tvergaard, V., "Plastic Buckling of Axially Compressed Cylindrical Shells," *International Journal of Thin-Walled Structures*, Vol. 1, 1983, pp. 139–163.

[7]Tvergaard, V., "On the Transition from a Diamond Mode to an Axisymmetric Mode of Collapse in Cylindrical Shells," *International Journal of Solids and Structures*, Vol. 19, No. 10, 1983, pp. 845–856.

[8]Mikkelsen, L. P., "Elastic–Viscoplastic Buckling of Circular Cylindrical Shells Under Axial Compression," *European Journal of Mechanics, A/Solids*, Vol. 14, No. 6, 1995, pp. 901–920.

[9]Koiter, W. T., "Buckling and Post-Buckling Behaviour of a Cylindrical Panel Under Uniaxial Compression," National Luchtvaart Lab., 20, Rept. S476, Amsterdam, May 1956.

[10]Koiter, W. T., "Over de stabiliteit van het elastisch evenwicht," Thesis, Delft, The Netherlands, 1945; also English Translations NASA TT-F10, 1967, and Air Force Flight Dynamics Lab., AFFDL-TR-70-25, Feb. 1970.

[11]Tvergaard, V., "Buckling of Elastic–Plastic Cylindrical Panel Under Axial Compression," *International Journal of Solids and Structures*, Vol. 13, 1977, pp. 957–970.

[12]Tvergaard, V., and Needleman, A., "Buckling Localization in a Cylindrical Panel Under Uniaxial Compression," *International Journal of Solids and Structures*, Vol. 37, 2000, pp. 6825–6842.

[13]Christoffersen, J., and Hutchinson, J. W., "A Class of Phenomenological Corner Theories of Plasticity," *Journal of the Mechanics and Physics of Solids*, Vol. 27, No. 5/6, 1979, pp. 465–487.

[14]Sanders, J. L., "Plastic Stress–Strain Relations Based on Linear Loading Functions," *Proceedings 2nd U.S. National Congress of Applied Mechanics*, Univ. of Michigan, Ann Arbor, MI, 1954, pp. 453–460.

[15]Ravn-Jensen, K., and Tvergaard, V., "Effect of Residual Stresses on Plastic Buckling of Cylindrical Shell Structures," *International Journal of Solids and Structures*, Vol. 26, No. 9/10, 1990, pp. 993–1004.

[16]Koiter, W. T., "On the Nonlinear Theory of Thin Elastic Shells," *Proceedings van het Koninklijke Nederlandse Akademie van Wetenschappen*, Vol. B69, Amsterdam, 1966, pp. 1–54.

[17]Niordson, F. I., *Shell Theory*, Series in Applied Mathematics and Mechanics, Vol. 29, North-Holland, Amsterdam, 1985, pp. 1–408.

[18]Hutchinson, J. W., "Plastic Buckling," *Advances in Applied Mechanics*, Vol. 14, 1974, pp. 67–144.

[19]Christoffersen, J., and Hutchinson, J. W., "A Class of Phenomenological Corner Theories of Plasticity," *Journal of the Mechanics and Physics of Solids*, Vol. 27, No. 5/6, 1979, pp. 465–487.

[20]Needleman, A., and Tvergaard, V., "Aspects of Plastic Postbuckling Behavior," *Mechanics of Solids*, Rodney Hill 60th Anniversary Volume, edited by H. G. Hopkins and M. J. Sewell, Pergamon, Oxford, 1982, pp. 453–498.

[21]Tvergaard, V., "Effect of Thickness Inhomogeneities in Internally Pressurized Elastic–Plastic Spherical Shells," *Journal of the Mechanics and Physics of Solids*, Vol. 24, 1976, pp. 291–304.

[22]Masubuchi, K., *Analysis of Welded Structures (Residual Stresses, Distortion, and their Consequences)*, Pergamon, Oxford, 1980, Fig. 8.1, pp. 328–335.

A. N. Palazotto
Associate Editor